

Heavy-quark production in two-photon collisions

M. Drees^{a,1}, M. Krämer^{b,c}, J. Zunft^b and P.M. Zerwas^b

^a *Physics Department, University of Wisconsin, Madison, WI 53706, USA*

^b *Deutsches Elektronen-Synchrotron DESY, W-2000 Hamburg 52, FRG*

^c *Institut für Physik, Johannes Gutenberg-Universität, W-6500 Mainz, FRG*

Received 26 February 1993, revised manuscript received 2 April 1993
Editor: P.V. Landshoff

Heavy quarks are copiously produced in two-photon collisions at e^+e^- colliders. We present the inclusive production rates and the final state distributions of the quarks, including QCD radiative corrections for the leading subprocesses. The results are compared with recent measurements of charmed particle production at PETRA and PEP, and predictions are given for TRISTAN and LEP energies.

1. Basic set-up

A large number of equivalent photons is generated at high-energy e^+e^- colliders, giving rise to the production of heavy-quark pairs in two-photon collisions. This process has been studied recently again for charmed particles in two experiments [1,2] after earlier measurements had reported rather strong threshold enhancements. The experimental analyses have been based theoretically on the direct production channel $\gamma\gamma \rightarrow c\bar{c}$ in the Born approximation. In this note we improve on the analysis of this process in two ways, (i) by taking into account radiative QCD corrections for the direct production process, and (ii) by including the contributions from resolved photons. It turns out that the QCD corrections increase the cross section significantly while the additional contributions from resolved photons are less important at collider energies of about 30 GeV. This picture remains qualitatively the same at LEP energies, though the 1-resolved γ mechanism becomes increasingly important with rising energy. Underneath the Z peak at LEP it is difficult to extract a clean sample of $\gamma\gamma$ events [3]. At LEP II, and similarly at TRISTAN, the very large number of $\gamma\gamma$ events, in turn, pose potential background problems to rare annihilation processes [4]. To get these reactions under proper control, we have extended the predictions to collider energies up to 200 GeV^{#1}. At the theoretical level the analysis overlaps to some extent with the photoproduction of heavy quarks at HERA which has been discussed thoroughly in ref. [9]. Where comparisons are possible for the virtual and soft gluon corrections we have found agreement with the calculations of ref. [9].

Three mechanisms contribute to the production of heavy quarks in $\gamma\gamma$ collisions; generic diagrams are shown in fig. 1.

¹ Heisenberg Fellow.

^{#1} The yield of heavy quarks at high energy e^+e^- linear colliders depends crucially on the spectrum of beamstrahl photons that varies strongly with the machine design, see e.g. ref. [5] where a (disfavored) broad-band design had been selected. The interesting case of top-quark production has been investigated, through the direct channel only, in refs. [6,7] parallel to this study. $\gamma\gamma$ production of c , b , t quarks has also been discussed at 500 GeV for beamstrahl photons and photons generated by laser back-scattering in ref. [8].

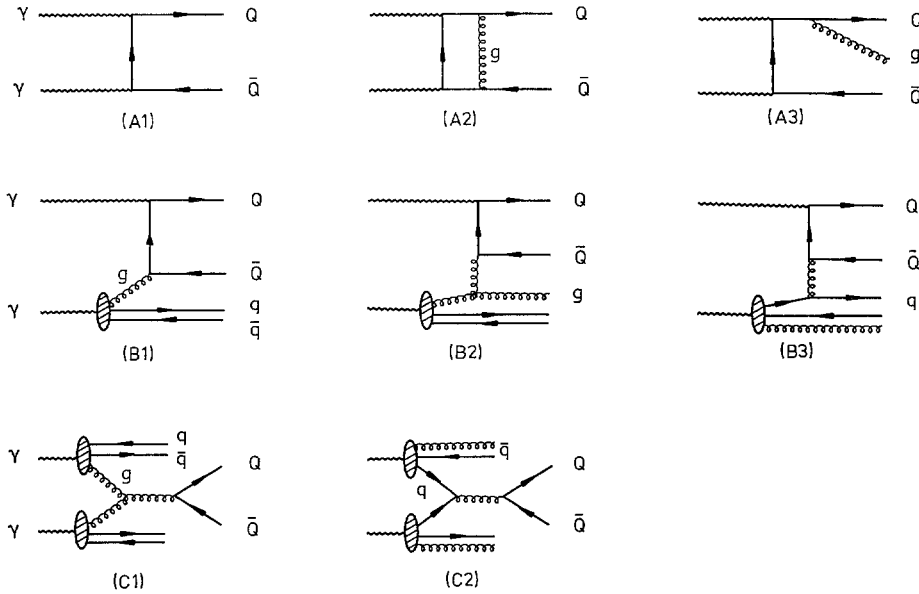


Fig. 1. Generic diagrams for heavy-quark production in $\gamma\gamma$ collisions. (A) direct production, (B) one photon resolved, and (C) two photons resolved.

(i) In the case of direct production (A), the photons couple directly to the heavy quarks. No spectator particles travel along the γ axes. At the Born level the cross section is given by [10]

$$\sigma_0(\gamma\gamma \rightarrow Q\bar{Q}) = \frac{4\pi\alpha^2 e_Q^4 N_c}{s_{\gamma\gamma}} \left[\left(1 + \frac{4m_Q^2}{s_{\gamma\gamma}} - \frac{8m_Q^4}{s_{\gamma\gamma}^2} \right) \log \frac{1+\beta}{1-\beta} - \beta \left(1 + \frac{4m_Q^2}{s_{\gamma\gamma}} \right) \right], \tag{1}$$

where $s_{\gamma\gamma}$ denotes the total $\gamma\gamma$ energy squared and $\beta = (1 - 4m_Q^2/s_{\gamma\gamma})^{1/2}$ the velocity of the quark Q . The calculation of the QCD corrections follows the standard procedure. The differential cross sections, including virtual plus soft gluon corrections and hard gluon radiation, can be determined analytically [9]^{#2}. The (regularized) exchange of coulombic gluons between the final state quarks gives rise to a β^{-1} singularity in the production probability which compensates the phase space factor β ,

$$\sigma(\gamma\gamma \rightarrow Q\bar{Q}(g)) = \frac{4\pi\alpha^2 e_Q^4 N_c}{s_{\gamma\gamma}} \beta \left\{ 1 + \frac{4\alpha_s}{3\pi} \left[\frac{\pi^2}{2\beta} - \left(5 - \frac{\pi^2}{4} \right) + \mathcal{O}(\beta) \right] \right\}. \tag{2}$$

This final state interaction in the color singlet $Q\bar{Q}$ channel is attractive. Multiple gluon exchange sums up to the Sommerfeld coefficient $\frac{4}{3} (\pi\alpha_s/\beta) \{1 - \exp[-\frac{4}{3} (\pi\alpha_s/\beta)]\}^{-1}$ before isolated $(Q\bar{Q})$ resonances form at still lower energies. The QCD corrected cross section is non-zero at the threshold, accounting on average for the production of $J = 0$ $Q\bar{Q}$ resonances.

The predictions for the direct production channel do not depend on quark and gluon distributions in the photon so that they are free of phenomenological parameters. They depend only on the heavy-quark mass and the QCD coupling constant. The final result may be summarized, most conveniently for numerical evaluations, in the form

^{#2} A detailed comparison of the numerically integrated total cross section has been performed together with the authors of ref. [6] and agreement has been found mutually between the results.

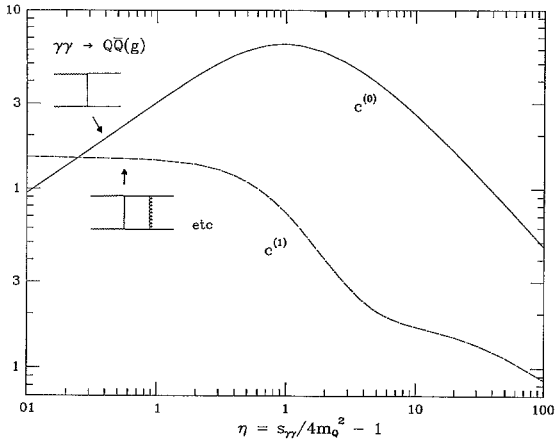


Fig. 2. Coefficients of the QCD corrected total cross section for $\gamma\gamma \rightarrow Q\bar{Q}(g)$ in the physically relevant range of the scaling variable $s_{\gamma\gamma}/4m_Q^2$.

$$\sigma(\gamma\gamma \rightarrow Q\bar{Q}(g)) = \frac{\alpha^2 e_Q^4}{m_Q^2} (c_{\gamma\gamma}^{(0)} + 4\pi\alpha_s c_{\gamma\gamma}^{(1)}), \tag{3}$$

where the functions $c_{\gamma\gamma}^{(0,1)}$ depend only on the ratio $\rho = s_{\gamma\gamma}/4m_Q^2$. They are shown in fig. 2 for the relevant range of ρ values within the \overline{MS} scheme; the heavy-quark mass is defined in the on-mass-shell scheme.

(ii) If one of the photons first splits into a flux of light quarks and gluons [11], one of the gluons may fuse with the second photon to form the $Q\bar{Q}$ pair (fig. 1.B1). The remaining light quarks and gluons build up a spectator jet in the split γ direction (single resolved γ contribution). While the Born cross section can be derived from (1) by just replacing $\alpha^2 e_Q^4 \rightarrow \frac{4}{3}\alpha\alpha_s e_Q^2$ for the basic $g\gamma \rightarrow Q\bar{Q}$ subprocess, the total $\gamma\gamma$ cross section of this mechanism depends on the gluon density of the photon [12–14]. Since the number of gluons in the resolved photon grows $\sim \alpha\alpha_s^{-1}$, the resolved γ processes are of the same order as the direct process. Besides the virtual QCD corrections and the soft and hard gluon radiation (B2), the cross section in next-to-leading order involves also the subprocess $\gamma q \rightarrow Q\bar{Q}q$ (B3). (Final states with four heavy quarks are strongly phase space suppressed [15].) The QCD corrected cross sections of the subprocesses may be parametrized as

$$\sigma_{\gamma i} = \frac{\alpha\alpha_s e_Q^2}{m_Q^2} \left[c_{\gamma i}^{(0)} + 4\pi\alpha_s \left(c_{\gamma i}^{(1)} + \bar{c}_{\gamma i}^{(1)} \log \frac{\mu^2}{m_Q^2} \right) \right] \quad (i = g, q), \tag{4}$$

where the coefficients $c_{\gamma g}$ and $c_{\gamma q} = \hat{c}_{\gamma q} + (e_q/e_Q)^2 d_{\gamma q}$ as functions of $s_{\gamma i}/4m_Q^2$ can be found in ref. [9]; μ is the renormalization and factorization scale which we identify in this analysis. In addition to the repulsive coulombic final state interaction in the $Q\bar{Q}$ octet state generated in the $g\gamma$ subprocess, logarithmic singularities occur near threshold due to soft initial-state gluon radiation,

$$\begin{aligned} \sigma(\gamma g \rightarrow Q\bar{Q}(g)) \\ = \frac{2\pi\alpha\alpha_s e_Q^2}{s_{\gamma g}} \beta \left[1 + \frac{\alpha_s}{\pi} \left(-\frac{1}{12} \frac{\pi^2}{\beta} + 3 \log^2 8\beta^2 - 15 \log 8\beta^2 - 3 \log 4\beta^2 \log \frac{\mu^2}{m_Q^2} + \mathcal{O}(\beta) \right) \right]. \end{aligned} \tag{5}$$

Very close to the threshold multiple gluon exchange leads to Sommerfeld's exponential suppression factor $-(\pi\alpha_s/6\beta) [1 - \exp(\pi\alpha_s/6\beta)]^{-1} \simeq (\pi\alpha_s/6\beta) \exp(-\pi\alpha_s/6\beta)$ [16].

For the quark and gluon densities of the photon we adopt the Drees–Grassie (DG) [12] and the Gluck–Reya–Vogt (GRV) [13] parametrizations. The latter are particularly suited to characterize the magnitude of the radiative corrections properly. They allow us to compare the results for the Born cross section folded with leading order parton densities, with the cross sections consistently evaluated for parton cross sections and parton densities in next-to-leading order.

(iii) If both photons split into quarks and gluons (C), the $Q\bar{Q}$ pair is accompanied by two spectator jets (double resolved γ contribution). It turns out a posteriori that, for the energies analyzed in this note, the double resolved γ contribution, given in Born approximation [17] by

$$\sigma(gg \rightarrow Q\bar{Q}) = \frac{\pi\alpha_s^2}{3s} \left[\left(1 + \frac{4m_Q^2}{s} + \frac{m_Q^4}{s^2} \right) \log \frac{1+\beta}{1-\beta} - \frac{\beta}{4} \left(7 + \frac{31m_Q^2}{s} \right) \right], \quad (6)$$

$$\sigma(q\bar{q} \rightarrow Q\bar{Q}) = \frac{8\pi\alpha_s^2}{27s} \beta \left(1 + \frac{2m_Q^2}{s} \right), \quad (7)$$

is much smaller than the direct and the single resolved γ contributions. This had been observed previously in ref. [18] for the energy range covered by TRISTAN. From the analysis of heavy-quark production in hadron collisions we conclude that QCD corrections [19] cannot change this order-of-magnitude suppression significantly and we will not take into account QCD corrections for this channel.

For the spectrum of the Weizsäcker–Williams photons we will adopt the standard form [10]

$$n(z) = \frac{\alpha}{2\pi} \frac{1 + (1-z)^2}{z} \log \frac{Q_{\max}^{\text{eff}}}{Q_{\min}^2}, \quad (8)$$

with $Q_{\min}^2 = m_c^2 z^2 / (1-z)$; Q_{\max}^{eff} is expected to be somewhat smaller than the maximum virtualness of the photon. By comparing the exact result for $e^+e^- \rightarrow e^+e^-c\bar{c}$ in the Born approximation [20] with the equivalent photon approximation, we find that for $Q_{\max}^{\text{eff}} = Q_{\max}^2/4 = (W_{\gamma\gamma}^2 - 4m_Q^2)/4$ the discrepancy is less than 3%. This cut-off value should also provide a solid basis for the calculation of the cross section including QCD corrections.

2. Results

We present the final results for the inclusive production of heavy quarks in two steps.

(i) The energy dependence of the total cross sections for the production of charm and bottom quarks $e^+e^- \rightarrow e^+e^-c\bar{c}/b\bar{b}(g)$ is shown in figs. 3a, 3b. The cross sections are given in next-to-leading order with the renormalization / factorization scale set to the average transverse mass $\mu = \sqrt{2}m_Q$ (for $\langle p_{\perp} \rangle \sim m_Q$), and $A^{(4)} = 340$ MeV in the $\overline{\text{MS}}$ scheme; the quark masses, defined in the on-mass-shell renormalization scheme, are chosen as $m_c = 1.6$ GeV and $m_b = 4.75$ GeV. The open $c\bar{c}$ and $b\bar{b}$ threshold energies are set to 3.8 GeV and 10.6 GeV, respectively. The vertical bars attached to the curves indicate how much the values of the cross sections are altered if μ varies between $m_Q/2$ (1.3 GeV for c) and $2m_Q$ (left bars) ^{#3}, and if the quark masses vary between 1.3/1.8 GeV and 4.5/5.2 GeV for c and b quarks, respectively (right bars). The GRV parametrization has been adopted for the quark and gluon densities of the photon.

From fig. 3, and from the detailed numbers collected in table 1, we can draw the following conclusions. At

^{#3} In contrast to heavy-quark production in hadron collisions we expect a small variation of the resolved- γ cross sections with μ at the Born level since the μ fall-off of the parton cross section [$\sim \alpha_s^k(\mu^2)$] is neutralized asymptotically by the increasing number of gluon and quark partons in the photons ($\sim [\alpha_s^{-1}(\mu^2)]^k$, $k = 1$ or 2 for 1- or 2-resolved γ).

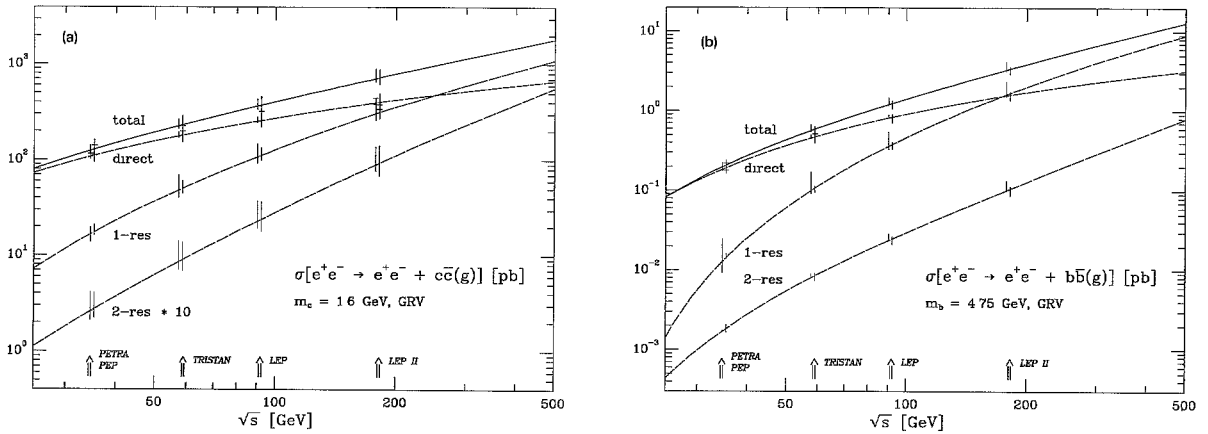


Fig. 3. Total cross sections for $e^+e^- \rightarrow e^+e^- + Q\bar{Q}(g)$ as functions of the e^+e^- collider energy, (a) charm; and (b) bottom quarks. The total cross sections are broken down to the direct and resolved γ contributions. Parameters: $m_c = 1.6$ GeV, $m_b = 4.75$ GeV, $A_{MS}^{(4)} = 340$ MeV, $\mu = \sqrt{2}m_Q$; $\sqrt{s_{\gamma\gamma}} \geq 3.8$ GeV (charm), 10.6 GeV (bottom); GRV [13] parton parametrizations, EPA spectrum eq. (8). The left bars indicate the change of the cross sections if the renormalization scale is varied between $m_Q/2$ (1.3 GeV for c) and $2m_Q$, the right bars if the c -, b -quark masses are varied between 1.3/1.8 and 4.5/5.2 GeV, respectively.

Table 1

Comparison of the cross sections, evaluated for two different parton parametrizations and cuts in the transverse momentum and rapidity of the c , b quarks. Also shown is the K factor defined as $K = \sigma_{NLO}/\sigma_{LO}$ which characterizes the higher order corrections. Parameters as in fig. 3

	E (GeV)	Q	Direct	1-resolved		Total	
				GRV	DG	GRV	DG
σ_{LO} (pb)	180	c	296.8	269.9	228.3	575.9	530.5
		b	1.280	1.371	1.232	2.754	2.571
	91.2	c	191.2	93.38	75.85	286.9	268.6
		b	0.663	0.302	0.249	0.989	0.924
σ_{NLO} (pb)	180	c	396.3	305.8	315.1	711.3	716.8
		b	1.582	1.644	1.576	3.329	3.217
	91.2	c	254.8	109.5	100.9	366.7	357.3
		b	0.823	0.371	0.301	1.218	1.136
K	180	c	1.335	1.133	–	1.235	–
		b	1.236	1.199	–	1.209	–
	91.2	c	1.333	1.173	–	1.278	–
		b	1.241	1.228	–	1.232	–
σ_{NLO} (pb) $ y \leq 1.7$ $p_{\perp} \geq 5$ GeV	180	c	8.243	6.603	5.065	14.93	13.37
		b	0.415	0.418	0.359	0.857	0.787
	91.2	c	4.426	1.873	1.312	6.318	5.752
		b	0.222	0.106	0.076	0.333	0.301

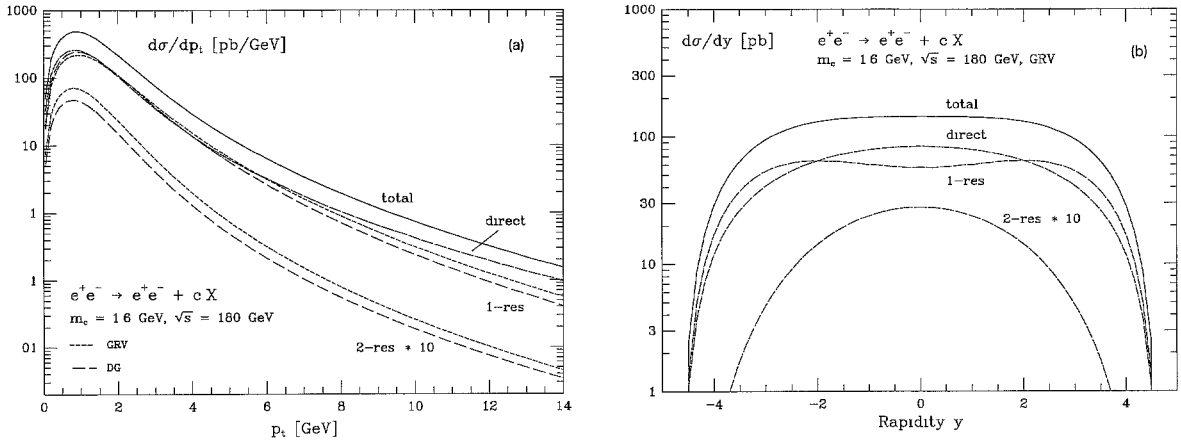


Fig. 4. Transverse momentum and rapidity distributions in $e^+e^- \rightarrow e^+e^- + cX$ for LEP II at the c -quark level.

low energies in the PETRA/PEP/TRISTAN range, the direct production mechanism by far dominates the total cross section. At LEP II ~ 180 GeV, the direct contribution and the 1-resolved γ contribution are of equal size. The cross sections for charmed particle production are large, giving a total of $\sim 350\,000$ events for an integrated luminosity of $\int \mathcal{L} = 500 \text{ pb}^{-1}$ at LEP II; b quark production is suppressed by more than two orders of magnitude. A cut on the angular distribution / rapidity of $|y| \leq 1.7$ for the c quark reduces the cross sections by approximately 50%. However, even if the transverse momentum is cut at $p_\perp \geq 5$ GeV, we are left with a very large number of charm events, $\sim 10\,000$ $c\bar{c}$ pairs at LEP II.

The QCD radiative corrections are very important, increasing the cross sections by $\sim 30\%$. This can best be demonstrated by examining the K factors, $K = \sigma_{\text{NLO}}/\sigma_{\text{LO}}$, where all quantities, cross sections of the subprocesses and parton distributions, are consistently calculated in next-to-leading and leading order, respectively. Since the direct production is dominating, the theoretical predictions do not depend much on the quark and gluon densities of the photon. Barring extreme parametrizations, the uncertainties can be characterized properly by comparing the GRV [13] results with the earlier DG [12] parametrizations. The predictions of the total cross sections appear to be theoretically firm.

Cuts on the Q transverse momenta enlarge the differences in the 1-resolved γ contribution between various parton parametrizations. However, since the dominant weight of the direct production mechanism becomes even more pronounced at large transverse momenta, the overall distributions remain insensitive. Transverse momentum and rapidity distributions are displayed for charm quarks at LEP II in figs. 4a, 4b. The plateau for charm production, generated by the plateau of the equivalent γ distribution, extends for LEP II over eight units of rapidity. The shape of the distributions for b quarks is similar to those of the charm quarks.

(ii) PETRA and PEP data on charmed particle production in $\gamma\gamma$ collisions at 35 and 29 GeV e^+e^- collider energies have been reanalyzed recently. From the measured cross sections for semiinclusive $D^{*\pm}$ production, table 2, the total charm production cross section has been extracted by the TASSO and the TPC/2 γ Collaborations [1,2]. Even though the statistical and systematic errors are large, the measured charm cross sections appear to overshoot the values estimated at the Born level consistently. Adding however the QCD radiative corrections to the Born term and including the resolved γ contributions, the agreement with the recent experimental analyses [1,2] is quite satisfactory.

An estimate of charmed particle $\gamma\gamma$ production near threshold, that includes exclusive channels, has been attempted in ref. [1], resulting – if taken at face value – in a cross section fifteen times larger than predicted in the Born approximation. It is clear that the QCD corrections considered here, cannot account for an increase

Table 2

Comparison of the measured seminclusive charm production cross sections at PETRA and PEP with the theoretical QCD predictions.

	Measured values $\sigma(e^+e^- \rightarrow e^+e^-D^{*\pm}X)$	Born (pb)	QCD corrections [%] direct/1-resolved/2-resolved	Total (pb)
TASSO [1]	97 ± 29	46		67
TPC/2 γ [2]	74 ± 26	43	24/18/0.3	62

by an order of magnitude, nor could other QCD based mechanisms [15] get close to this estimate. Diffractive channels which may build up the celebrated $\rho^0\rho^0$ enhancement, cannot contribute to $D\bar{D}$ final states either. However the experimental estimate is based on several extrapolations and auxiliary assumptions leading to systematic errors which cannot be controlled properly. We are therefore tempted to conclude that the analysis in ref. [1] grossly overestimates the $\gamma\gamma$ cross section for charmed particle production near the threshold.

3. Conclusion

Seminclusive heavy-quark production in $\gamma\gamma$ collisions at e^+e^- colliders can reliably be predicted in QCD. The recent D^* charm data from PETRA and PEP are accounted for in a satisfactory way. A large yield of charm quarks – even if cuts on the transverse momenta are applied – is predicted from the TRISTAN throughout the LEP II energy range.

Acknowledgement

We are grateful to our experimental colleagues A. Finch and D. Miller from LEP for their enthusiastic encouragement. We acknowledge detailed comparisons of part of the results with the authors of ref. [6]. We have greatly benefitted from a discussion with U. Karshon on the uncertainties in experimental estimates of $\gamma\gamma$ charmed-particle production near threshold. M.K. is grateful to the German Bundesministerium für Forschung und Technologie and J.Z. thanks Professor A. Wagner at DESY for providing financial support.

References

- [1] TASSO Collab., W. Braunschweig et al., Z. Phys. C 47 (1990) 499.
- [2] TPC/2 γ Collab., M. Alston-Garnjost et al., Phys. Lett. B 252 (1990) 499.
- [3] L. Bergstrom, I. Bigi, M. Drees and T. Sjostrand, in: Report of the Working Group on High luminosities at LEP, CERN 91-02.
- [4] D.J. Miller et al., in: ECFA Workshop on LEP200 (Aachen, 1986), report CERN 87-08.
- [5] F. Halzen, C.S. Kim and M.L. Stong, Phys. Lett. B 274 (1992) 489.
- [6] J.H. Kuhn, E. Mirkes and J. Steegborn, Karlsruhe preprint TTP92-28.
- [7] I.I. Bigi, F. Gabbiani and V.A. Khoze, preprint SLAC-PUB 5951.
- [8] O.J.P. Eboli, M.C. Gonzales-Garcia, F. Halzen and S.F. Novaes, Madison preprint MAD-PH-701 (revised).
- [9] J. Smith and W. van Neerven, Nucl. Phys. B 374 (1992) 36.
- [10] See e.g. S.J. Brodsky, T. Kinoshita and H. Terazawa, Phys. Rev. D 4 (1971) 1532.
- [11] T.F. Walsh and P.M. Zerwas, Phys. Lett. B 44 (1973) 195,
E. Witten, Nucl. Phys. B 120 (1977) 189
- [12] M. Drees and K. Grassie, Z. Phys. C 28 (1985) 451.
- [13] M. Gluck, E. Reya and A. Vogt, Phys. Rev. D 46 (1992) 1973.

- [14] L.E. Gordon and J.K. Storrow, *Z. Phys. C* 56 (1992) 307;
H. Abramowicz, K. Charchula and A. Levy, *Phys. Lett. B* 269 (1991) 458.
- [15] S.J. Brodsky, G. Köpp and P.M. Zerwas, *Phys. Rev. Lett.* 58 (1987) 443.
- [16] For a recent discussion see V. Fadin, V.A. Khoze and T. Sjöstrand, *Z. Phys. C* 48 (1990) 613
- [17] M. Gluck, J.F. Owens and E. Reya, *Phys. Rev. D* 17 (1978) 2324.
- [18] M. Drees and R. Godbole, *Nucl. Phys. B* 339 (1990) 355.
- [19] P. Nason, S. Dawson and R.K. Ellis, *Nucl. Phys. B* 303 (1988) 607;
G. Altarelli, M. Diemoz, G. Martinelli and P. Nason, *Nucl. Phys. B* 308 (1988) 724;
W. Beenakker, H. Kuijf, W. van Neerven and J. Smith, *Phys. Rev. D* 40 (1989) 54.
- [20] V.M. Budnev, I.F. Ginzburg, G. Meledin and V. Serbo, *Phys. Rep.* 15 (1975) 181,
F.A. Berends, P.H. Daverfeldt and R. Kleiss, *Phys. Lett. B* 148 (1984) 489.